

Supplement of Atmos. Chem. Phys., 18, 14175–14196, 2018
<https://doi.org/10.5194/acp-18-14175-2018-supplement>
© Author(s) 2018. This work is distributed under
the Creative Commons Attribution 4.0 License.



Supplement of

Atmospheric processing of iron in mineral and combustion aerosols: development of an intermediate-complexity mechanism suitable for Earth system models

Rachel A. Scanza et al.

Correspondence to: Rachel A. Scanza (rachel.scanza@pnnl.gov)

The copyright of individual parts of the supplement might differ from the CC BY 4.0 License.

5 **Table S1:** Mass fractions of iron-containing minerals (Journet et al., 2008) and their apportionment to readily released, medium soluble, and slow soluble iron.

	FE_{Total}	FE_{RR}	FE_{Med}	FE_{Slow}
Hematite	57.50%			57.50%
Smectite	11.00%	0.55%	10.45%	
Illite	4.00%	0.11%	3.90%	
Feldspar	0.34%	0.01%		0.33%
Kaolinite	0.24%	0.01%		0.23%

10

15

20

Table S2a: Global annually-averaged atmospheric loading for REF and SS1-6.

Load	REF	SS1	SS2	SS3	SS4	SS5	SS6
Dust (Tg/yr)	16.1	16.1	16.1	16.1	16.1	16.1	16.1
Fe_{total} (Tg/yr)	0.6	0.6	0.6	0.6	0.5	0.6	0.6
Fes_{med} (Gg/yr)	15.1	6.7	14.5	1.7	11.1	15.8	15.2
Fes_{slow} (Gg/yr)	0.2	0.1	0.2	n/a	0.2	0.3	0.3
Fet_{comb} (Gg/yr)	14.5	14.5	14.5	14.5	14.5	14.5	14.5
Fes_{comb} (Gg/yr)	1.2	0.8	1.0	1.0	1.2	1.4	1.3

Table S2b: Global annually-averaged wet deposition for REF and SS1-6

Wet Dep.	REF	SS1	SS2	SS3	SS4	SS5	SS6
Dust (Tg/yr)	637.9	637.9	637.9	638.6	637.9	637.9	637.9
Fe_{total} (Tg/yr)	23.8	23.8	23.8	22.4	20.5	23.8	23.8
Fes_{med} (Gg/yr)	912.4	269.6	887.3	181.1	693.9	954.8	929.9
Fes_{slow} (Gg/yr)	13.4	2.8	12.8	n/a	12.8	19.2	18.6
Fet_{comb} (Gg/yr)	1142.7	1142.7	1142.7	1142.7	1142.7	1142.7	1142.7
Fes_{comb} (Gg/yr)	90.8	55.6	84.4	97.7	90.7	103.6	97.5

5 **Table S2c:** Global annually averaged dry deposition for REF, SS1-6.

Dry Dep.	REF	SS1	SS2	SS3	SS4	SS5	SS6
Dust (Tg/yr)	1143.4	1143.3	1143.3	1146.1	1143.4	1143.4	1143.4
Fe_{total} (Tg/yr)	33.5	33.5	33.5	40.1	36.8	33.5	33.5
Fes_{med} (Gg/yr)	351.9	284.3	358.9	25.2	402.5	359.8	366.8
Fes_{slow} (Gg/yr)	2.2	0.8	2.3	n/a	2.2	3.8	3.8
Fet_{comb} (Gg/yr)	756.1	756.1	756.1	756.1	756.1	756.1	756.1
Fes_{comb} (Gg/yr)	37.6	32.6	36.6	36.8	37.6	40.9	39.9

10

15

Table S2d: Global annually-averaged emissions for REF, SS1-6.

Emission	REF	REF_{bin1}	SS1	SS2	SS3	SS4	SS5	SS6
Dust (Tg/yr)	1767.8	19.3	1767.7	1767.6	1771.1	1767.7	1767.8	1767.8
Fe_{total} (Tg/yr)	56.9	1.0	56.9	56.9	62.0	56.9	56.9	56.9
Fes_{med} (Gg/yr)	506.9	35.9	506.9	506.9	0.0	506.9	506.9	506.9
Fes_{slow} (Gg/yr)	0.0	0.0	0.0	0.0	0.0	0.0	0.0	0.0
Fet_{comb} (Gg/yr)	1878.9	241.6	1878.9	1878.9	1878.9	1878.9	1878.9	1878.9
Fes_{comb} (Gg/yr)	75.2	9.7	75.2	75.2	75.2	75.2	75.2	75.2

5 **Table S2e:** Total deposition (Gg/yr) for ocean regions defined as Western North Pacific (WNP) (40-60°N, 140-185°E) and Eastern North Pacific (ENP) (40-60°N, 185-230°E) for SS1 to compare to Table 6 from (Ito and Xu, 2014).

Dep	WNP	ENP
Dust (Gg/yr)	6162.0	2747.6
Fe_{total} (Gg/yr)	237.9	108.8
Fes_{med} (Gg/yr)	3.3	1.7
Fes_{slow} (Gg/yr)	0.05	0.03
Fet_{comb} (Gg/yr)	30.7	6.3
Fes_{comb} (Gg/yr)	1.4	0.3

10

15

20

25

Table S3a: Global annually-averaged atmospheric loading for preindustrial (PI) cases 1-4.

Load	PI1	PI2	PI3	PI4
Dust (Tg/yr)	16.1	10.0	10.0	10.0
Fe_{total} (Tg/yr)	0.6	0.4	0.4	0.4
Fes_{med} (Gg/yr)	13.1	8.1	8.1	7.8
Fes_{slow} (Gg/yr)	0.12	0.08	0.08	0.07
Fet_{comb} (Gg/yr)	14.5	14.5	8.5	8.5
Fes_{comb} (Gg/yr)	1.0	1.0	0.6	0.6

Table S3b: Global annually-averaged wet deposition for PI1-4.

Wet Dep.	PI1	PI2	PI3	PI4
Dust (Tg/yr)	637.9	406.7	406.7	406.7
Fe_{total} (Tg/yr)	23.8	15.1	15.1	15.1
Fes_{med} (Gg/yr)	772.1	486.5	486.5	474.0
Fes_{slow} (Gg/yr)	9.8	6.3	6.3	6.1
Fet_{comb} (Gg/yr)	1142.7	1142.6	601.8	601.8
Fes_{comb} (Gg/yr)	79.1	79.5	43.1	41.5

5

Table S3c: Global annually-averaged dry deposition for PI1-4.

Dry Dep.	PI1	PI2	PI3	PI4
Dust (Tg/yr)	1143.4	705.3	705.2	705.2
Fe_{total} (Tg/yr)	33.5	20.7	20.7	20.7
Fes_{med} (Gg/yr)	337.9	210.7	210.7	211.5
Fes_{slow} (Gg/yr)	1.5	1.0	1.0	1.0
Fet_{comb} (Gg/yr)	756.1	756.2	410.1	410.1
Fes_{comb} (Gg/yr)	35.5	35.6	19.3	19.0

10

15

Table S3d: Global annually-averaged emissions for PI1-4.

Emission	PI1	PI2	PI3	PI4
Dust (Tg/yr)	1767.7	1103.6	1103.6	1103.5
Fe_{total} (Tg/yr)	56.9	35.5	35.5	35.5
Fes_{med} (Gg/yr)	506.9	316.8	316.8	316.8
Fes_{slow} (Gg/yr)	0.0	0.0	0.0	0.0
Fet_{comb} (Gg/yr)	1878.9	1878.9	1001.7	1001.7
Fes_{comb} (Gg/yr)	75.2	75.2	40.1	40.1

5

10

15

20

25

30

35

Table S4: Latitude and longitude of 12 ocean basins as defined by Gregg et al., 2003.

	Latitude	Longitude
N.Atlantic	lat>=30	lon<=75 lon>270
N.Pacific	lat>=30	lon>75 & lon<=270
N.Cen.Atl.	lat>=10 & lat<30	lon>270
N.Cen.Pac.	lat>=10 & lat<30	lon>120 & lon<=270
N.Indian.Ocn	lat>=10 & lat<30	lon>30 & lon<=120
Equat.Atl.	lat>=-10 & lat<10	lon<=30 lon>300
Equat.Pac.	lat>=-10 & lat<10	lon>120 & lon<300
Equat.In.Ocn.	lat>=-10 & lat<10	lon>30 & lon<120
S.Atlantic	lat>=-30 & lat<10	lon<=30 lon>300
S.Pacific	lat>=-30 & lat<-10	lon>120 & lon<=300
S.Indian.Ocn	lat>=-30 & lat<-10	lon>30 & lon<=120
Antarctic	lat<-30	lon>0 & lon<=360

5

10

15

20

25

30

Table S5a: Global ocean and regional ocean basin total fractional iron solubility (dust + combustion) for REF, SS1-6.

	Ref	SS1	SS2	SS3	SS4	SS5	SS6
Global	3.26	1.20	3.14	0.86	2.82	3.49	3.37
N.Atlantic	2.06	1.03	2.30	0.43	1.80	2.15	2.39
N.Pacific	4.92	1.83	5.39	2.48	4.46	5.49	5.95
N.Cen.Atl.	2.96	1.07	3.07	0.72	2.48	3.08	3.19
N.Cen.Pac.	6.49	2.35	6.93	2.61	5.70	7.83	8.26
N.Indian.Ocn	1.98	0.99	2.17	0.44	1.87	2.12	2.32
Equat.Atl.	7.06	1.36	5.05	1.66	6.53	7.35	5.34
Equat.Pac.	9.37	2.93	8.63	4.29	8.56	11.08	10.37
Equat.In.Ocn.	3.79	1.59	4.06	1.20	3.24	4.30	4.57
S.Atlantic	5.62	2.47	4.53	2.86	5.01	6.56	5.50
S.Pacific	5.40	3.11	5.10	4.07	5.44	6.67	6.39
S.Indian.Ocn	7.23	3.44	6.31	4.58	6.95	8.70	7.79
Antarctic	2.92	1.57	2.75	1.68	2.91	3.39	3.22

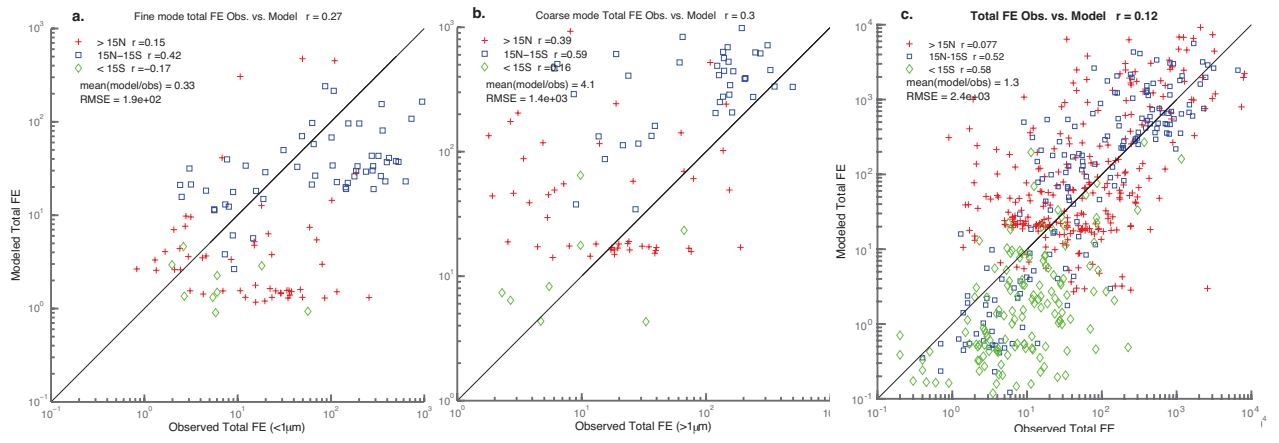
Table S5b: Global ocean and regional ocean basin total fractional iron solubility for preindustrial simulations.

	PI1	PI2	PI3	PI4
Global	2.80	2.87	2.77	2.72
N.Atlantic	1.93	1.97	1.92	2.01
N.Pacific	4.26	4.14	3.95	3.92
N.Cen.Atl.	2.75	2.81	2.80	2.86
N.Cen.Pac.	5.62	5.17	5.02	5.15
N.Indian.Ocn	1.78	1.81	1.76	1.77
Equat.Atl.	5.22	5.40	5.26	4.59
Equat.Pac.	8.05	8.25	7.95	7.85
Equat.In.Ocn.	3.30	3.37	3.10	3.10
S.Atlantic	4.50	4.26	3.98	3.79
S.Pacific	4.88	5.21	5.07	5.01
S.Indian.Ocn	6.05	6.07	6.13	5.88
Antarctic	2.66	3.02	3.02	3.00

5

10

Figure S1: Scatter plots of model total iron vs. observed total iron for fine mode, coarse mode and for fine + coarse mode.



5

10

15

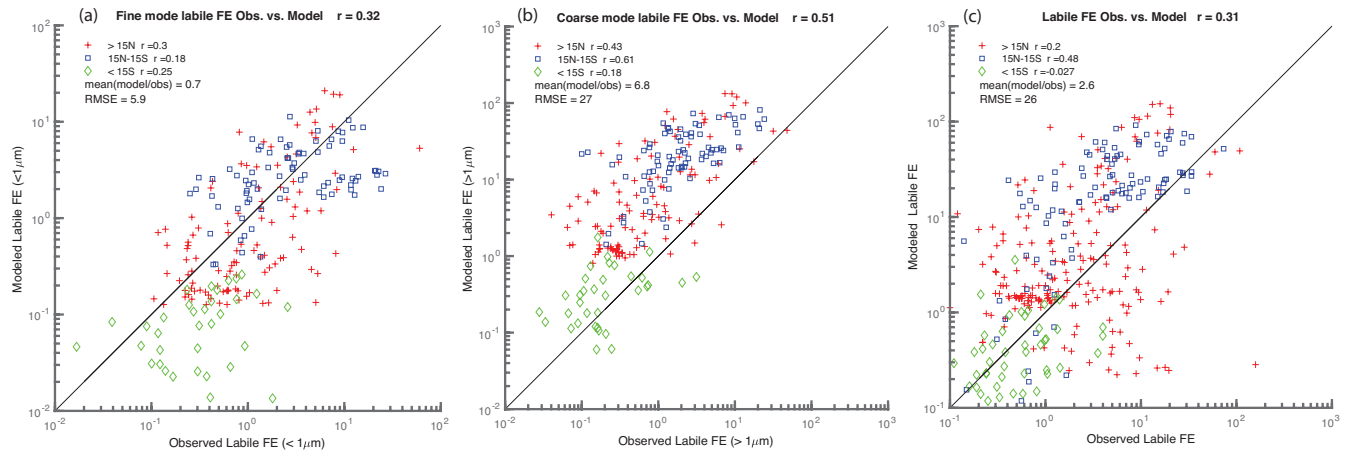
20

25

30

35

Figure S2: Scatter plots of model labile iron vs. observed labile iron for fine mode, coarse mode and for fine + coarse mode.



5

10

15

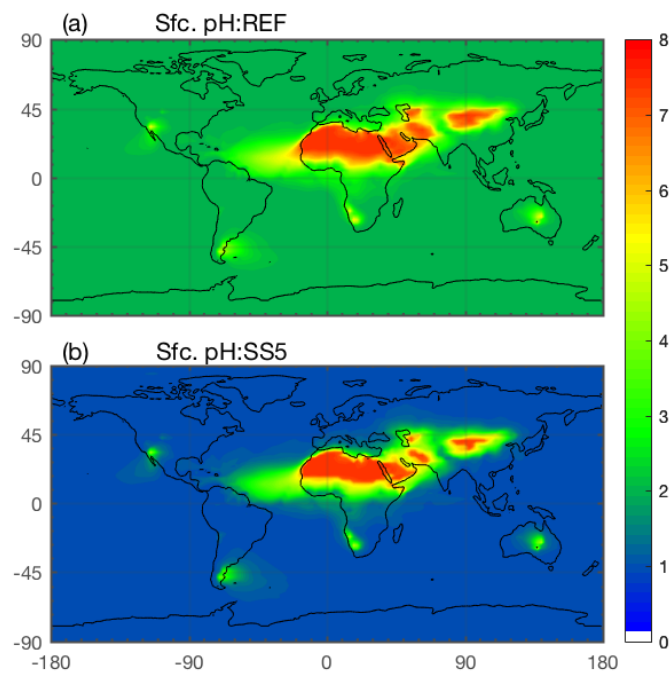
20

25

30

35

Figure S3: Spatial distribution of annual averaged pH at the surface for the reference case **(a)** and SS5 **(b)**.

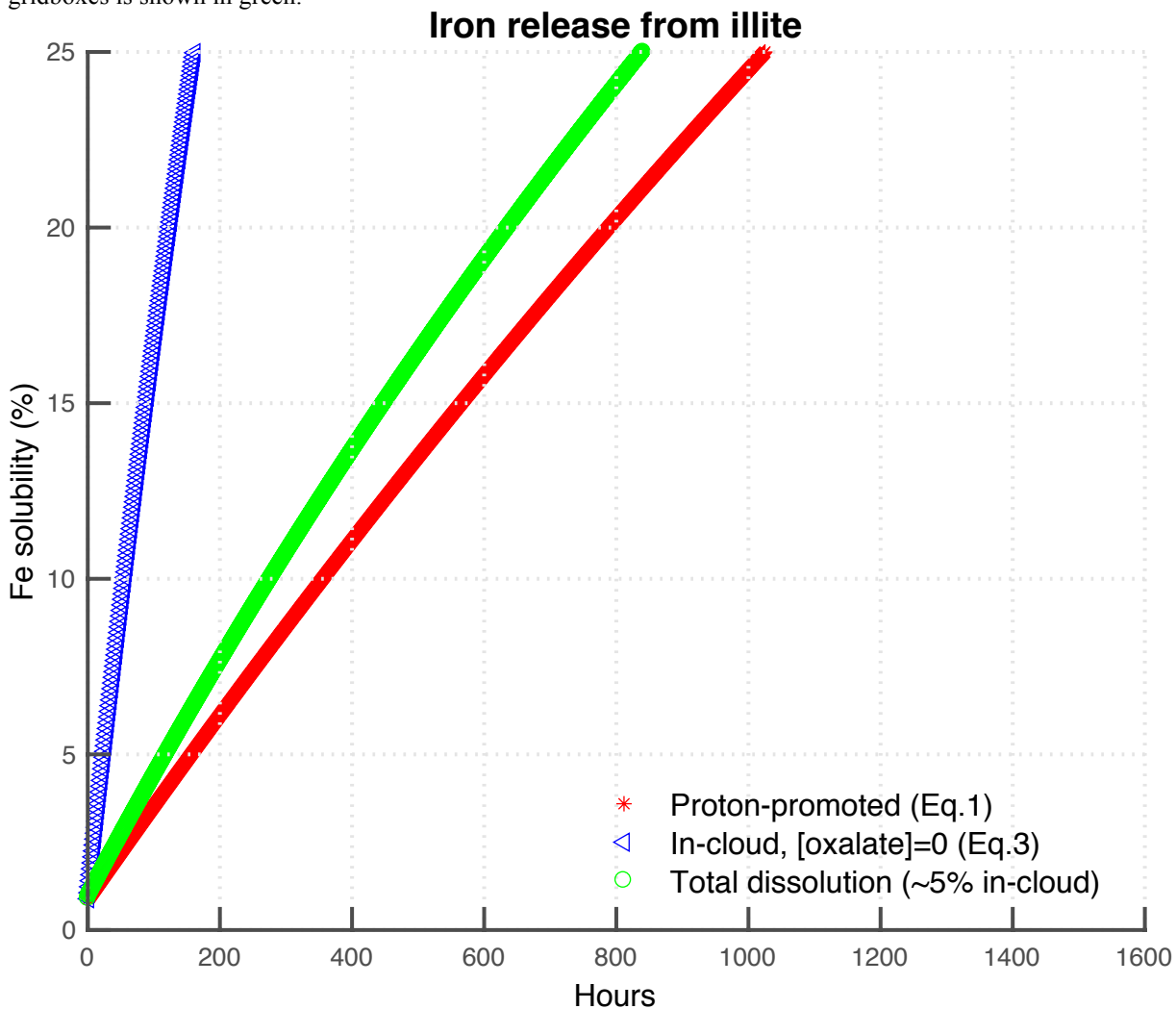


5

10

15

Figure S4: Percent iron solubility from medium soluble iron (Fe_{med}) at $pH = 2$, $T=298 \text{ }^\circ K$ (for comparison with Figure S2 from Ito and Shi, 2016). Proton-promoted dissolution applied at all model gridboxes is calculated from Eq. (1) and is shown in red. The iron liberation from in-cloud, organic ligand processing at $[C_2O_4^{2-}] = 0$ is shown in blue and is only applied in the cloud-fraction of gridboxes within clouds given by Eq. (3). The total iron dissolution for $\sim 5\%$ in-cloud to all atmosphere gridboxes is shown in green.



10

15

5 **Figure S5:** Fractional iron solubility (%) versus total iron concentration (ng m^{-3}) for the three cases considered in Box 2, Mahowald et al., 2018. For the combustion case (blue), the iron present in dust and combustion aerosols contribute to the total iron but only the iron within smaller combustion aerosols (fine mode) is soluble. The simple atmospheric processing case (green) assumes that aerosol iron gradually becomes more soluble with time while the third case (red) assumes that atmospheric iron processing occurs due to a pollutant (acidic species) emitted simultaneously with aerosol iron whose concentration decreases with time. This can be directly compared to Panel (b) in Box 2 from Mahowald et al., 2018 but is shown on a linear scale to enable a visual comparison to Figure 3 in Sholkovitz et al., 2012.

